THE AMERICAN MINERALOGIST, VOL. 56, JANUARY–FEBRUARY, 1971

TEXTURE VARIATIONS IN COLOR-ZONED TOURMALINE CRYSTALS

C. E. WAGNER, C. O. POLLARD, JR., R. A. YOUNG,
Georgia Institute of Technology, Atlanta, Georgia 30332 AND
GABRIELLE DONNAY, *Geophysical Laboratory, Carnegie Institution of Washington, Washington, D. C.*

ABSTRACT

Two X-ray diffraction imaging techniques have been applied for the first time to the study of previously unnoted mosaic detail in color-zoned Brazilian tourmaline. The divergence source-image distortion (DSID) technique gives maximum values for misorientations among all observable grains, whereas the convergence source-image distortion (CSID) technique yields the magnitude of misorientation between adjacent grains. Strikingly abrupt textural changes are observed; they are always accompanied by color changes. The converse is not found to hold. The central or core region of all five plates studied shows a macromosaic texture corresponding to an intrinsic rocking curve that would have a width at half height of ~1.2 minutes of arc. No grain elongation is observed.

The core region is sharply delineated from a surrounding ring or overgrowth region of lamellar texture, in which grains approximate $(2\bar{1}\bar{1}0)$ lamellae. The lattices of the lamellae in a given region are tilted with respect to each other by angles predominantly less than 5 minutes of arc but ranging up to 13 minutes of arc, the tilt axis being parallel to the long dimension of the lamella in the basal plane. The lamellar grains are subparallel in a given boundary region, and are normal to the growth boundaries on the $(01\bar{1}0)$, $(\bar{1}010)$ $(\bar{1}100)$ faces but on the other three regions they are parallel to the lamellae on an adjacent boundary. Electron microprobe traces rule out exsolution and compositional domain structures as an explanation of lamellar texture. Sudden drastic changes in conditions controlling crystal growth are possible causes of our observations.

INTRODUCTION

Textural variations have been observed in tourmaline (Wagner, Donnay, Pollard, and Young, 1968) by a special X-ray technique, source-image distortion (SID) (Young and Wagner, 1966). The variations of interest were those between different homogenous textures in adjacent regions of single crystals showing color zones. Abrupt texture changes are always accompanied by color changes, but the converse is not true.

The possibility that characteristic texture-differences, not indicated by other methods, may be related to one or more parameters (such as growth temperature and pressure) is suggested on the basis of the work reported here which also includes lattice-parameter measurements, electron-microprobe analyses, optical studies in polarized light, and X-ray radiography.

SID Technique because the source-image distortion (SID) technique (Young and Wagner, 1966) is not widely known, a brief summary follows, together with a description of a new modification of the technique.

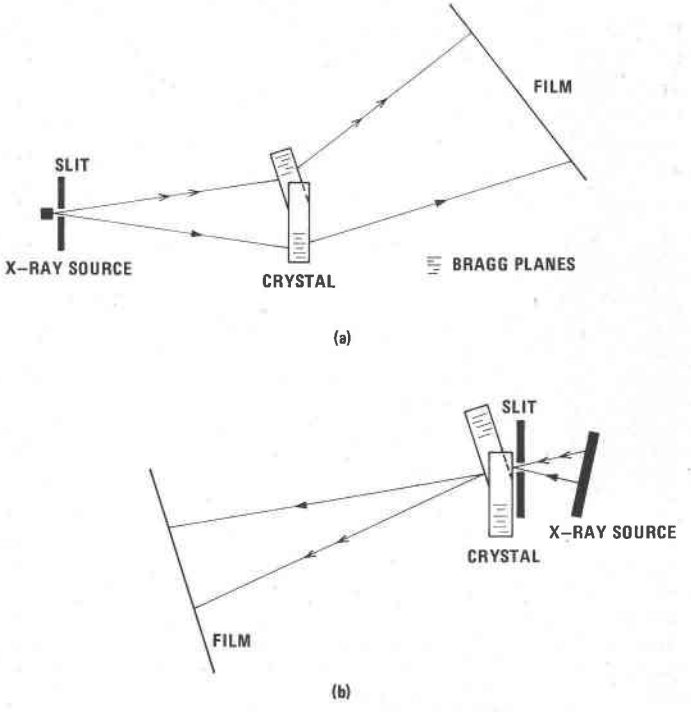

FIG. 1. (a) Divergence and (b) convergence SID arrangements.

Two different geometric arrangements were used. In both arrangements, the X-ray source has dimensions such that it extends only very slightly outside the plane of incidence (p.o.i.), the plane containing the incident and the scattered X-ray beam to be detected. (The normal to any diffracting set of Bragg planes also, of necessity, lies in the p.o.i.) In both arrangements sufficient cross-fire is present in the p.o.i. so that the incident beam simultaneously meets the condition for Bragg diffraction for crystal regions of slightly different orientations and interplanar spacings, d.

In the divergence SID technique (DSID) the source dimension in the p.o.i. and perpendicular to the source-to-specimen line is limited either by small source size or by a slit placed as close to the source as is conveniently possible. A variation of this arrangement uses a line source in the p.o.i. and Soller slits near the source to give the effect of several "point" sources. Thus the required cross-fire is provided in the form of divergence (Fig. 1a). In the convergence SID technique (CSID) arrangement, the source dimension measured in the p.o.i. is deliberately made large, e.g., the long dimension of a line-focus source of x-rays is placed in the p.o.i. and the limiting slit is placed as close to the specimen as possible. The required cross-fire is thereby provided as convergence (Fig. 1b).

The SID principle may be understood from consideration of either arrangement; the divergence arrangement is chosen for the more detailed discussion here. When a large planar crystal is placed in diffracting position at some distance from a point source of X rays, not all of the crystal can diffract the characteristic wavelength simultaneously. The loci of actively diffracting portions extend in a band across the crystal. The width of this band depends on the intrinsic diffraction profile of the crystal and on the dimension of

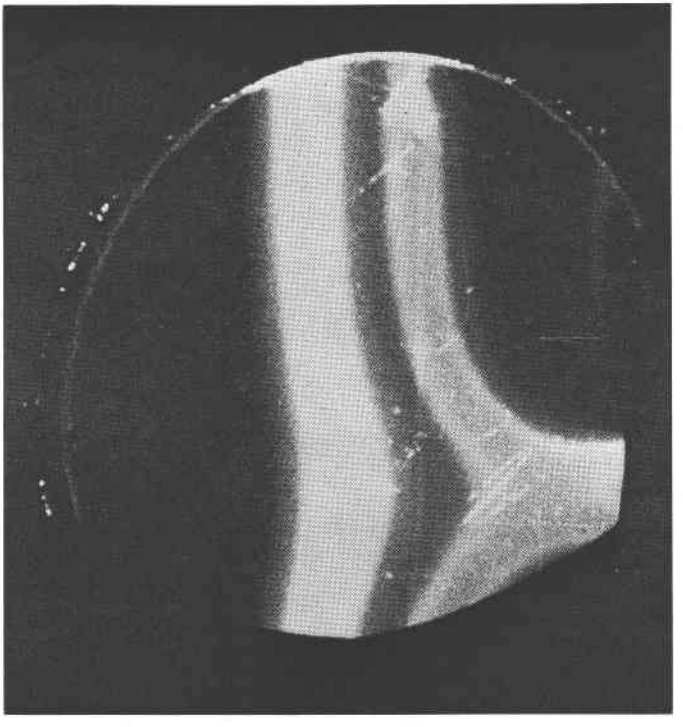

FIG. 2. Single source divergence SID pattern showing diffracting regions for $K\alpha_1$ and $K\alpha_2$ wavelengths. A bending of the crystal produced the deformation of the diffracting regions.

the X-ray source in the p.o.i. A film placed perpendicular to the diffracted beam at any point records the location of the diffracting regions as elongated "source images". Distortions in the crystal under examination, such as changes in lattice spacing or misalignment of grains, cause the region effectively diffracting the incident X-ray beam to be shifted across the face of the crystal (Fig. 2). It can be seen that $K\alpha_1$ and $K\alpha_2$ wavelengths are well resolved and diffract along separate bands. The band of one is badly distorted because it crossed over a region of the crystal that was warped by the mounting cement; the other one did not.

At each point, the shift of the diffracting band from its "normal" location is determined by the component of tilt about an axis normal to the p.o.i. or by the change in spacing of the active Bragg planes or by a combination of both. The angular change produced by a strain, $\Delta d/d$, increases with the tangent of the Bragg angle. The contributions of tilt and strain to the distortion of the image can, therefore, be separately determined from observations made with several orders of the same reflection. They also can be separated by observations with the pair of reflections hkl and $\bar{h}\bar{k}\bar{l}$ (strain will increase or decrease the apparent diffraction angle similarly for both reflections but tilt will increase the apparent diffraction angle for one and decrease it for the other.)

For crystals with narrow diffraction profiles, a single slit provides information for only a small fraction of the crystal surface. Several separate X-ray sources equally spaced along a line in the p.o.i. will have separate loci of reflection on the crystal and so may be used to

sample distortions over a larger area at once. Soller slits placed in front of a line source lying in the plane of incidence produce such an effect (Fig. 3). If no significant distortion is present in the specimen, the source image consists of parallel lines (Fig. 4).

In the CSID technique (not previously reported) the defining slit is placed adjacent to the sample with the slit extending normal to the p.o.i. so that the crystal is illuminated with convergent radiation. Each specimen point in the band defined by the slit can then diffract (when the crystal is "aligned"). The film records (Fig. 5) the direction in which the diffracted ray from each point travels (with respect to the rays diffracted from the other portions of the band) and over what angular range (width of diffraction profile). Typical dimensions are: slit width, 0.05 mm; X-ray-source-to-specimen distance, 12 cm (providing

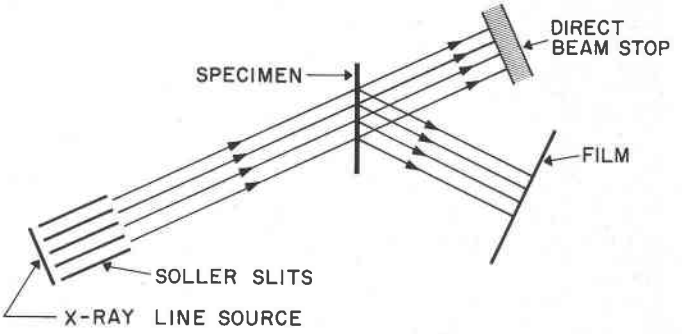

FIG. 3. Experimental arrangement for the multiple source, divergence SID experiment. Source-to-specimen distance is typically 1 meter. Each beam, indicated in the figure by a single line, is actually divergent to the degree permitted by the length and spacing of the Soller slits.

a maximum convergence angle of about 5 degrees); and specimen-to-film distance, 1 m or more (to provide good resolution of angular variations). Principally, the two methods differ in that, for DSID, the active source points are fixed and the selection of active specimen points depends on the distortions present, whereas for CSID, the slit determines the active specimen points and the distortions determine the active source points.

Definition of Texture. Texture shall be taken here to mean the pattern of grain size and orientation within what would ordinarily be called a single crystal. One extreme case is that of a nearly perfect, undistorted crystal, such as the quartz plate used for Fig. 4. For the more usual case of "single" crystals with relatively few randomly-oriented microcracks and low-angle grain boundaries (Fig. 6) we will use the term "macromosaic texture." In Figure 7 the grains are apparently elongated in at least one direction and misorientation occurs about an axis parallel to this direction. The texture of this sample will be referred to as "lamellar."

EXPERIMENTAL

General Characterization of the Tourmaline Specimens. Some "single" crystals of minerals show evidence of heterogeneity even to the naked eye. A well known example is that of multicolored tourmaline. Electron-microprobe analyses for Fe, Mn, Mg, and Al re-confirmed the correlation

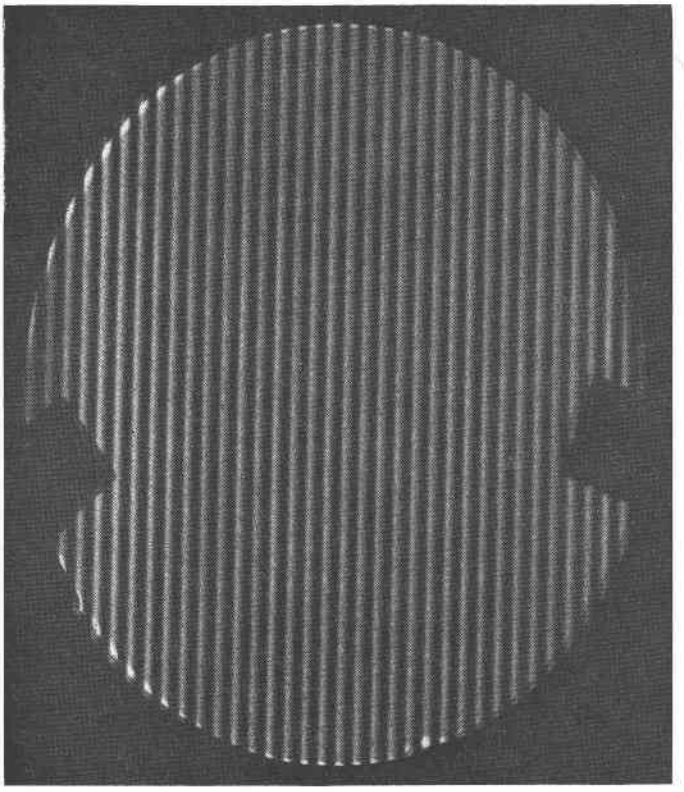

FIG. 4. Multiple source, divergence SID pattern of a perfect, undistorted quartz crystal.

between color and content of Fe and Mn first reported by Bradley and Bradley (1953) on the basis of spectroscopic analyses. However, whether the correlation is with the absolute amounts present or is with the Fe-to-Mn ratio is still not known. Qualitatively, the colors range from black to green to blue to clear to pink as the Fe-to-Mn ratio decreases.

Contact X-ray radiographs (Fig. 8) of our largest three samples show that differences in X-ray density coincide with the differences in color.

Changes in lattice parameters were determined from doubly-exposed X-ray photographs prepared as follows: After a precession photograph was made of one small region of the sample, the film cassette was raised slightly, the crystal was translated parallel to itself to expose a different region of interest, and a second photograph was made on the same film. Uncertainties due to film shrinkage were thereby eliminated. The method

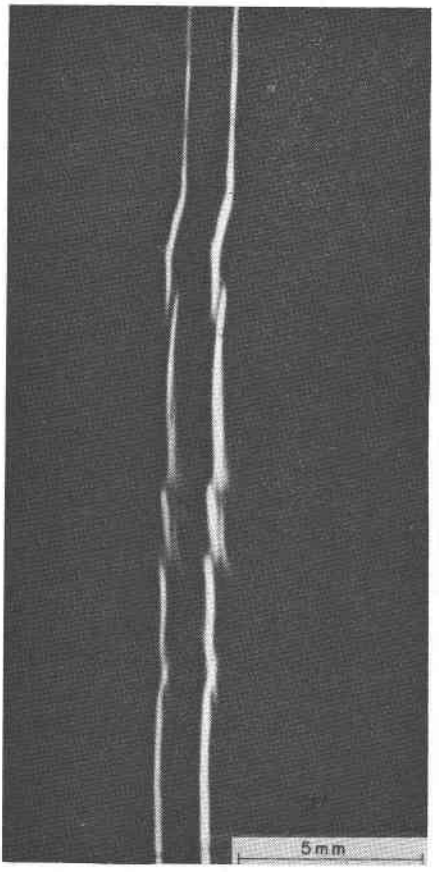

FIG. 5. Single slit, transmission, convergence SID pattern of a crystal exhibiting a discontinuity in the $K\alpha_1$ and $K\alpha_2$ images due to several small cracks. The $K\alpha_1$–$K\alpha_2$ separation is 2.8 minutes of arc. The slit in front of the specimen was 0.05 mm, the source-to-film distance 1 meter.

could also reveal misalignment between the exposed regions (Donnay, 1968). Two sections cut from one crystal of Brazilian tourmaline exhibiting a pink region and a blue region and sections from several other similar tourmaline crystals were so examined. Within a region of a single color, lattice-parameter differences of 0.4% were observed for a; between differently colored regions differences as large as 0.8% in a and 0.3% in c were observed, even though the samples appeared to be single crystals under the usual X-ray and optical examinations.

SID Studies of Tourmaline Crystals. Initial studies were undertaken to ascertain what, if any, strains accompanied the change in color (*i.e.*, in

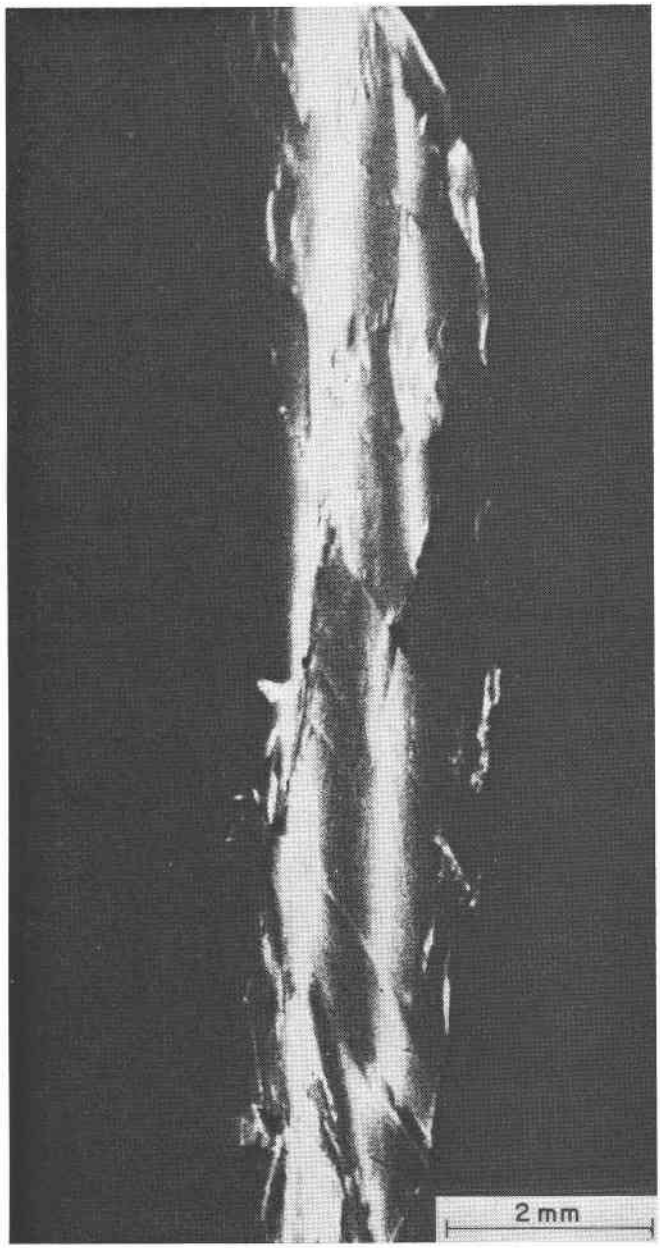

FIG. 6. Single slit, Bragg case, divergence SID pattern of a single grain exhibiting cracks and some broadening of the diffracted images of the $K\alpha_1$ and $K\alpha_2$ wavelengths.

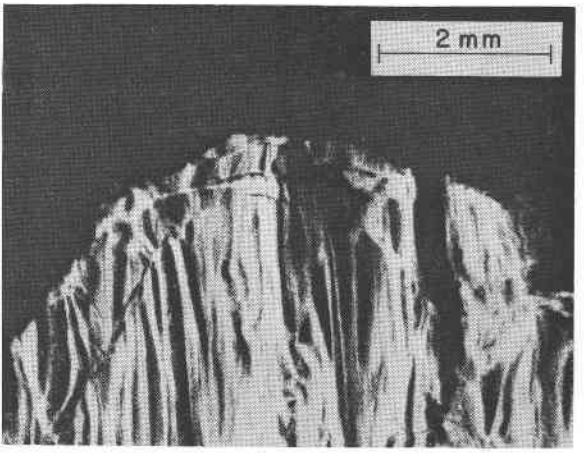

FIG. 7. Single slit, Bragg case, divergence SID pattern of a highly textured sample. This texture will later be identified as "lamellar".

chemical composition) at a color-zone boundary. DSID studies were made on (i) approximately 1 mm thick (00.1) sections of three tourmaline crystals of Brazilian origin (crystals B1–B3) and (ii) on a (00.1) section (B4) and a $(1\bar{2}.0)$ section (V1) so cut from the same Brazilian tourmaline crystal that they were nearly contiguous. B4 and V1 were about 0.2 mm thick.

All samples were polished and etched to remove surface strains. Each sample exhibited at least one strong color difference between color zones. Section B1 came from a crystal with a large blue core and a narrow clear rim. B2 came from a crystal color-zoned (from core to rim) dark green to pink to light green. B3 was cut from a crystal that had a core of one shade of pink over-grown with a zone of darker pink grading to light pink which, in turn, gave way to a medium-green rim. B4 and V1 were taken from a crystal that was zoned from light green in the center to pink to light green at the rim.

Sample B3. A 00.3 (symmetric Bragg case) DSID pattern of specimen B3 is shown in Figure 9. Two regions of distinctly different texture are detectable. In the central (pink) region of the specimen the $K\alpha_1$ and $K\alpha_2$ bands were slightly distorted in various directions as a consequence of the macromosaic texture. The diffracted images (the dark bands) were about 0.5 mm wide (unmagnified). Knowing the instrument dimensions, one could then deduce that the intrinsic rocking curve of this portion of the sample has a width at half height of about 3.6×10^{-4} radians or 1.2 minutes of arc.

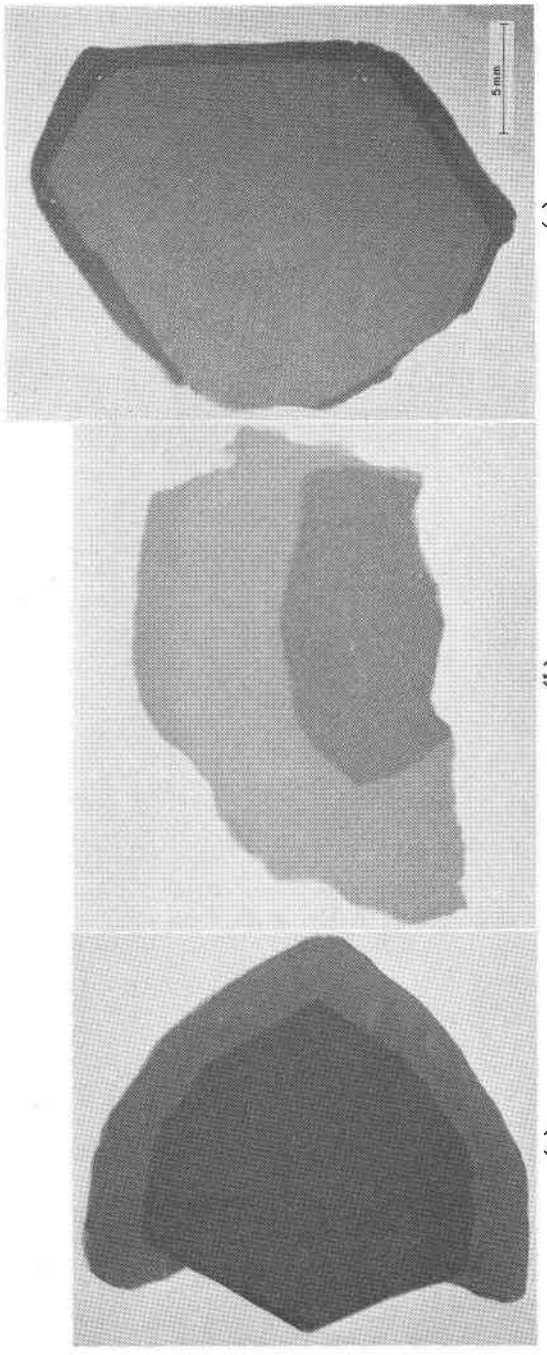

FIG. 8. X-ray radiographs of samples B1, B2, and B3. The X-ray source was a microfocus generator operating at 25 kv.

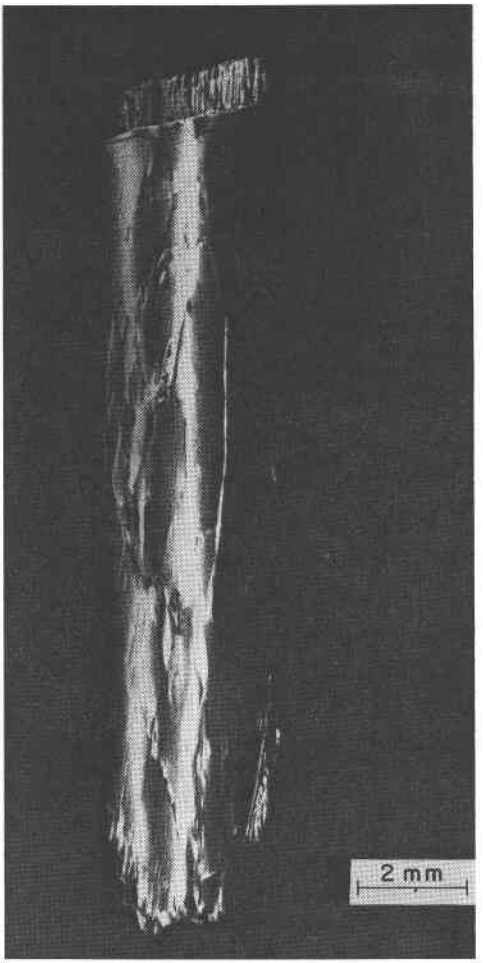

FIG. 9. Single slit 00.3 reflection (symmetric Bragg case), divergence SID pattern of specimen B3. The slit width was 0.08 mm, the source-to-specimen distance 134 cm, the crystal-to-film distance 3 cm, and the copper X-ray tube was operating at 50 kV.

From the character of the tip of the image, one sees, in the portion corresponding to the green region of the crystal, that the individual diffracting areas are much smaller than those in the pink region and that they are elongated and usually extend the entire width of the green region. Each individual distinct area of the image arises from a different grain, and we conclude that in this outer region the grains have an elongated dimension in the basal plane (00.1). These grains are shown below to be lamellae; therefore, this texture is designated "lamellar texture."

From patterns made with higher order reflections (00.6 and 00.9) it was determined that the distortions producing the characteristic textures are primarily tilts rather than strains. In any particular exposure the observable tilts were those with a component about an axis normal to the p.o.i. (*i.e.*, an axis parallel to the SID lines), as mentioned above; thus it could be determined from the DSID pattern of Figure 9 that the lamellar grains are misoriented, with a rotational component of 13 minutes of arc or less about a line parallel to the apparent elongation direction of the grains.

The crystal, B3, was then rotated 90° about the *c* direction and a 00.6 DSID pattern was obtained (Fig. 10). Since the same lamellar grains observed in Figure 9 are not delineated in Figure 10, it can be concluded that there are no significant misorientations about that axis which is (i) normal to the long direction of the grain image in Figure 9 and (ii) lies in the plane of the slice.

The other rim portions of this crystal yield similar results for their grains: (i) The grain cross-sections are elongated, (ii) in most cases the grains extend the entire width of the green region, (iii) the grains are misoriented about an axis approximately parallel to the long dimension of their observed cross-sections, and (iv) the angle of misorientation was usually not more than 5 minutes of arc and is very rarely more than 10 minutes of arc.

Samples B1 and B2. Similar results were obtained for the textures of the other basal sections, but a particular color could not be correlated with a particular texture. For instance, the lamellar-textured rim of B3 is light green and the central region is pink, but in specimen B2 lamellar textures were shown by both pink and light green rims about a dark green core. Cores never contained lamellar grains. Representative 00.3 DSID patterns of the three thicker samples (B1, B2, B3) are shown in Fig. 11.

The core regions often have roughly hexagonal cross-section in the basal plane, but the long dimensions of the grain cross-sections are perpendicular to the three overgrowth boundaries, (01.0), $(\bar{1}0.0)$ and $(1\bar{1}.0)$, but are not perpendicular to the $(0\bar{1}.0)$, (10.0) and $(\bar{1}1.0)$ boundaries. Instead, the lamellae on the latter three boundaries are parallel to the lamellae perpendicular to one of the adjacent overgrowth boundaries. On a given boundary there was but one orientation of the lamellar grains.

Sample B4. Sample B4 was thin enough to permit multiple source, transmission DSID patterns to be made without overlap of grain images (Fig. 12). The difference in textures between core and outer regions is

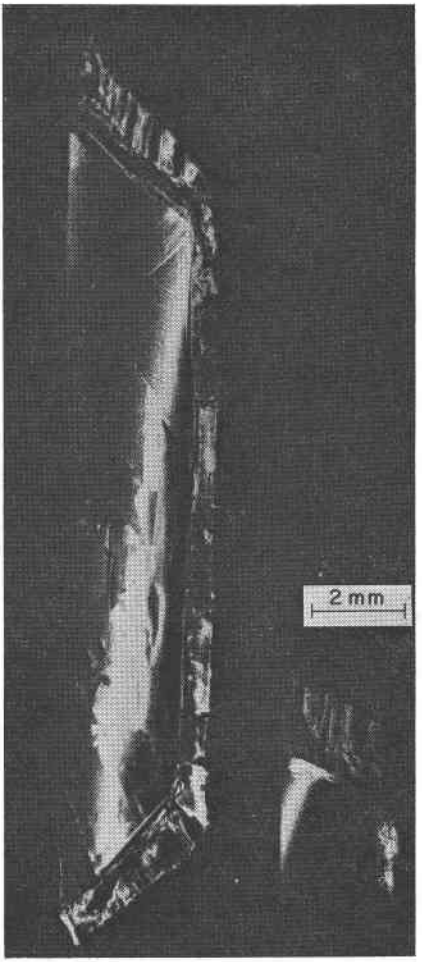

FIG. 10. Single slit, 00.6 reflection divergence SID pattern of specimen B3, with the p.o.i. rotated 90° about the surface normal from its position in Fig. 9. The lack of delineation of the grains on the right-hand edge in the figure, which was at the top of Fig. 9 means there is no misorientation of these grains about an axis parallel to that core-overgrowth boundary. (The second image in the lower right corner is a reflection from a different set of Bragg planes.)

more clearly shown here than in the preceding figures, as are the individual grains. However, the textures of this sample are similar to those of the other basal sections.

Sample V1. Because samples V1 and B4 were nearly contiguous, the extent of the rim grains in the *c* direction could be investigated. The ev-

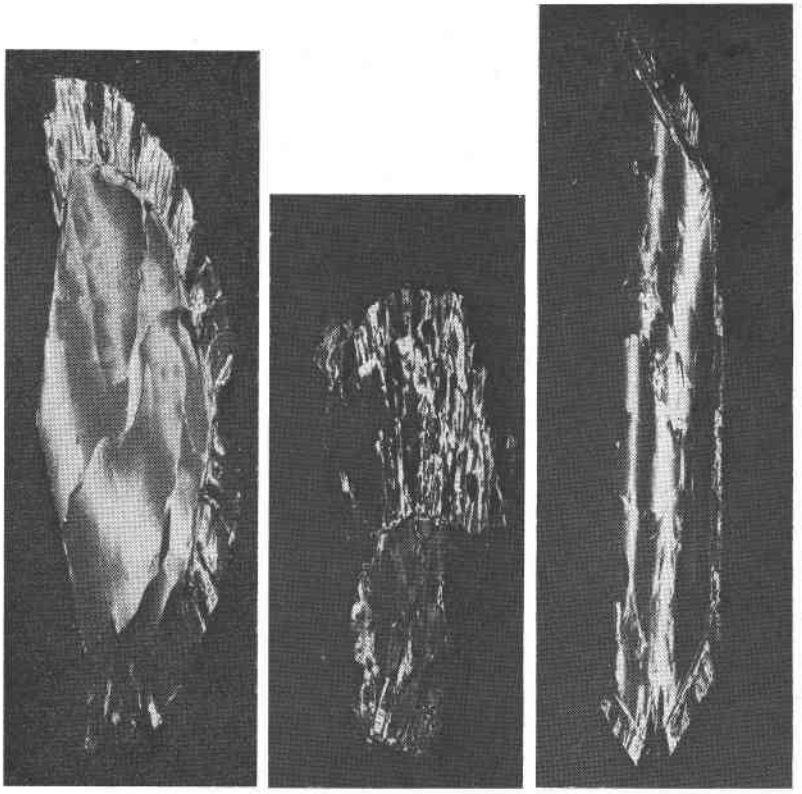

FIG. 11. Representative single slit, 00.3 reflections, divergence SID patterns of samples B1, B2, and B3 in approximately the same orientations as the crystals themselves in Fig. 8. Experimental conditions are the same as for Fig. 9. Magnification approximately 4.5×.

idence for the elongation parallel to c and for the lack of rotation about the c direction was obtained exclusively from this sample pair. Figure 13 is a multiple-source transmission DSID pattern of V1 obtained with the 33.0 reflection. The color and texture boundary observed in B4 occurs along a line joining the arrows, with the highly-textured rim region lying on the left. This sample has a large number of (optically)visible cracks which obscure the SID X-ray data. Near the left edge there are few, however, so the distortions of the SID lines there are due to other causes. To the left of the color boundary, striations of the SID lines similar to the ones observed in the top of Figure 12 are present. The misorientation between striated regions is less than 10 seconds of arc. Since the striations are similar in size and appearance to those in the basal section, it is assumed that they are the $(1\bar{2}.0)$ (vertical) cross-sections of the grains in

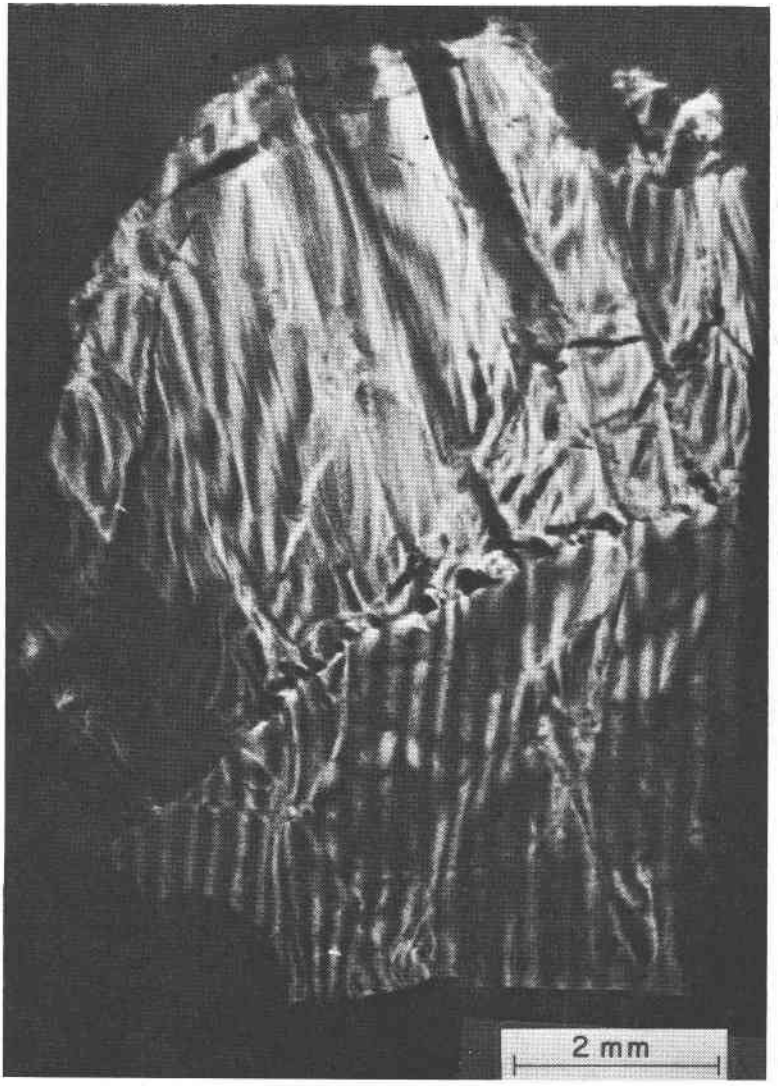

FIG. 12. Multiple source, 60.0 reflection (symmetric transmission), divergence SID pattern of sample B4. The source-to-crystal distance was 100 cm, and the crystal-to-film distance 15 cm. A high intensity molybednum target operating at 50 kV and 40 mA was used.

the basal plane. The absence of significant misorientations about the *c* direction indicates the only misorientation axis lies in the basal plane and further supports correlations wih the elongated grain cross-sections in Figure 12.

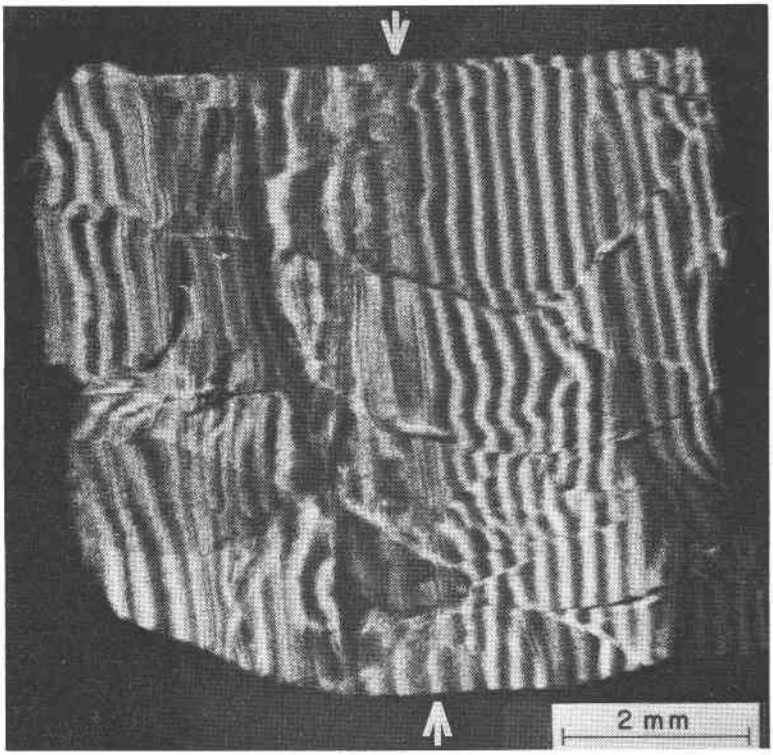

FIG. 13. Multiple source, 33.0 reflection (symmetric transmission), divergence SID pattern of sample V1 obtained under the same conditions as the pattern in Fig. 12. The *c*-axis is here vertical. The color change occurs along a line joining the arrows.

Model for textural variations. A model for the texture of the samples has thus been determined: there is, first, a core region with a macromosaic texture. Second, there is an overgrowth region having approximately the same crystallographic orientation as the core; however, the overgrowth region is composed of lamellar grains crystallographically misoriented with respect to each other by rotations of up to 13 minutes of arc but generally less than 5 minutes of arc about an axis lying in an a^* direction. The large dimensions of the lamellae lie in that a^* direction containing the axis of misorientation, and in the c direction. In specimen B4 and V1 the lamellae thicknesses are relatively uniform at about 0.04 mm.

Amount of lamellar tilt. Differences in orientation between adjacent lamellae were determined quantitatively with the CSID technique to see if any pattern of misorientation could be detected. None could be found. Basal sections were used, and the reflecting planes, p.o.i., and slit

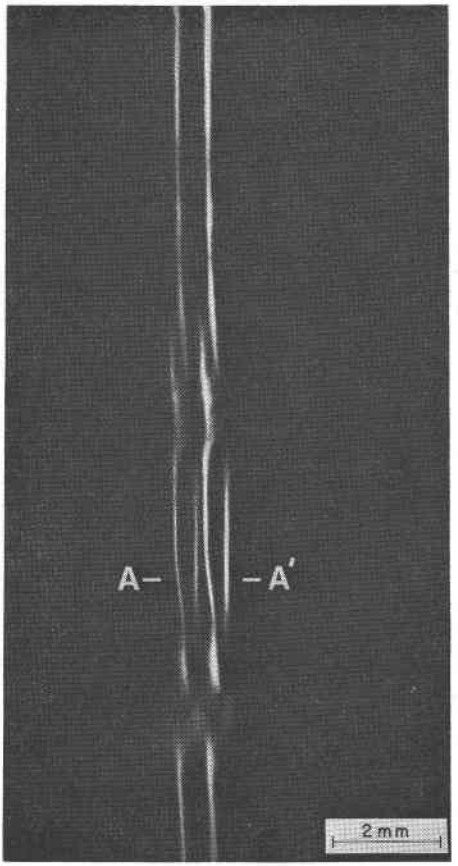

FIG. 14. Convergence SID pattern of specimen B4. Molybdenum $K\alpha_1$ and $K\alpha_2$ images for the 60.0 reflection are shown. The source-to-slit distance was 12 cm, crystal-to-film distance 100 cm, and the slit width was 0.05 mm.

orientations were chosen so that the lamellae made slight angles with the illuminated band. This configuration maximized the probability that a significant segment of the illuminated band would fall simultaneously on two neighboring lamellae. Near, maximum separation of the doubled images was achieved when the axis of misorientation was placed normal to the p.o.i. Only when two images for each wavelength were obtained from a segment of the illuminated band was it assumed that two different lamellae were diffracting; a simple discontinuity in an image could as readily be assigned to a crack within a lamella as to a simultaneous illumination of adjacent lamellae.

Figure 14 is a 60.0 CSID pattern of specimen B4. In Figure 14 ev-

idence for numerous cracks appears and numerous strained regions are indicated by slight widening of the line images. In the region between A and A′ two grains diffract simultaneously. Separations of images such as those at A-A′ constitute the proof of misorientation. Several CSID patterns were made, and all missorientations (approximately 10) so observed ranged from a minimum of 20 seconds to a maximum of 5 minutes of arc. The minimum detectable misorientation is approximately 10 seconds of arc. The CSID patterns reveal misorientations between adjacent lamellae, whereas misorientations reported from DSID patterns are maximum values for misorientations among all the lamellae.

Petrographic Observation of Lamellae. With the SID results in mind, one could discern the rim lamellae under the petrographic microscope, but only on specimen B2 (Fig. 15). Traces of the lamellae were discernible under crossed nicols when the traces were within several degrees of the 45° position to the polarization directions. Rotation of the stage, the polarizer, or the analyzer after the position of visibility was attained only decreased the resolution of the lamellae.

Visual correlation of lamellae observed by the SID method with those observed by optical methods was possible for limited portions of the rim. A complicating factor in this effort was the oblique projection angle for the images on the SID photographs. It was found that two slide projectors, from which the separate SID and optical images on suitable transparencies could be projected side-by-side from different focal lengths and different angles, were of great help in our efforts to correlate X-ray and optical images.

Discussion

The observation of greatest interest in this study is that two distinctly different textures are associated with specific regions of a "single" crystal. In each of the samples observed, the core region had a macromosaic texture containing some small cracks whereas the overgrowth region was composed of lamellar grains. No case was observed in which the core was composed of the lamellar grains, nor was a macromosaic region found as an overgrowth to a lamellar region.

Possible models consistent with the lamellar texture of the overgrowths include the following: (1) twin lamellae, (2) exsolution lamellae, (3) domain structures (including compositional domains; *e.g.*, sector zones), and (4) deformation lamellae. None is satisfactory. No twin operation with reasonably low indices could develop the sub-parallel aggregates of the lamellar regions. The possibility that the lamellar grains might be exsolution lamellae or compositional domains can be

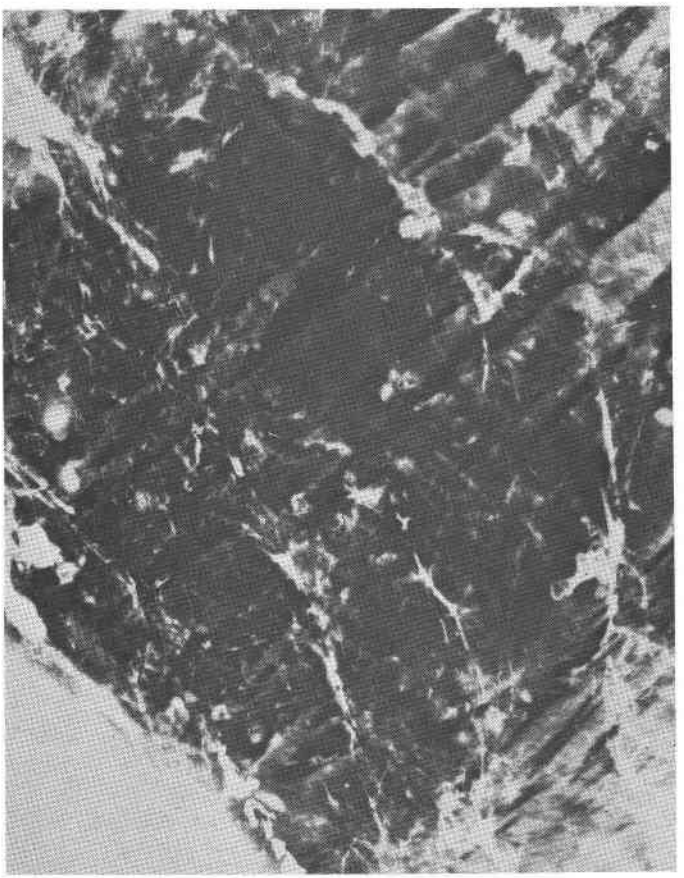

FIG. 15. Petrographic photomicrograph of specimen B4 between crossed Nicols. The color boundary is shown in the lower left corner. The suspected lamellar features are the bands that run from the lower left to the upper right corners. Magnification is approximately 43×.

ruled out on the basis of electron-microprobe traces (for Fe, Mn, Mg, and Al) made within lamellar regions of a single color. If exsolution or compositional domains had caused the lamellae, such traces would show a spatial dependence of chemical composition with the same repeat distance as the lamellae repeat distance. No such dependence was found with a 3 μm diameter microprobe beam. Domain structures other than compositional domains have not been ruled out; in fact, the lamellar texture could fairly be described as orientational-domain structure (which description gives no clue to the genesis). Deformation lamellae, such as have been reported in quartz (Bailey, Bell, and Peng, 1958) and

olivine (Challis, 1968), are mentioned as a possibility here only because of the similarity of their microscopic appearance to that of the rim lamellae. No suggestion that deformation might have given rise to the lamellae is intended, especially not in view of the orientations of the rim lamellae.

Color changes always accompany texture changes, but they also occur elsewhere. There appeared to be no strict correlation between a particular color and a particular texture. For example, in sample B2 the pink (overgrowth) region had the lamellar texture, whereas in B3 the pink (core) portion had the macromosaic texture. The microprobe work has shown the Fe-to-Mn ratio to be associated with color and the Mn and Al concentrations to have only small variations that are independent of color. The radiographs have shown that the absolute concentration of heavy elements is not associated with a particular texture. Thus it appears that chemical compositions, both relative and absolute, play a merely coincidentally associative, and not a causative, role in texture formation.

If the above possibilities are excluded, as they apparently should be, then texture must be indicative of some parameter to which the more established techniques, other than SID and related techniques, are not sensitive. One may then seriously entertain the conjecture that the texture changes are indicative of some growth parameter such as temperature, pressure, or others.

Acknowledgements

We thank Mr. Earl Williams of the Johns Hopkins University for supplying the tourmaline specimens and for cutting and polishing the plates. In the preparation of the manuscript, the efforts of the first three authors were partially supported by the U. S. Army Research Office-Durham.

References

Bradley, J. E. S., and Olive Bradley (1953) Observations on the coloring of pink and green zoned tourmaline. *Mineral. Mag.* **30,** 26–38.

Bailey, S. W., R. A. Bell, and C. J. Peng (1958) Plastic deformation of quartz in nature. *Geol. Soc. Amer. Bull.* **69,** 1443–1446.

Challis, G. A. (1968) X-ray study of deformation lamellae in olivines of ultramafic rocks. *Mineral. Mag.* **36,** 195–203.

Donnay, Gabrielle (1968) Crystalline heterogeneity: Evidence from electron-probe study of Brazilian tourmaline. *Carnegie Inst. Wash. Year Book* **67,** 219–220.

Wagner, C. E., G. Donnay, C. O. Pollard, Jr., and R. A. Young (1968) Textural variation in colored tourmaline crystals. *Amer. Crystallogr. Assoc. Meet. Abstr.* LL8.

Young, R. A., and C. E. Wagner (1966) X-ray source-image distortion technique for the study of crystal distortion and vibration. *J. Appl. Phys.* **37,** 4070–4076.

Manuscript received, July 1, 1970; accepted for publication, July 28, 1970.